Magnetic anisotropy in $(Er_xHo_{1-x})_xFe_{14}B$ pseudoternary intermetallic compounds

1993 J. Phys.: Condens. Matter 5 5637

(http://iopscience.iop.org/0953-8984/5/31/025)

J. Phys.: Condens. Matter 5 (1993) 5637–5648. Printed in the UK

Magnetic anisotropy in $(Er_xHo_{1-x})_2Fe_{14}B$ pseudoternary intermetallic compounds

M R Ibarra†, L Paretí‡, P A Algarabel†, L Morellon†, C Marquina† and M Solzi‡§

† Laboratorio de Magnetismo, Departamento de Física de la Materia Condensada and Instituto de Ciencia de Materiales de Aragón, Facultad de Ciencias, Universidad de Zaragoza—Consejo Superior de Investigaciones Científicas, 50009-Zaragoza, Spain

‡ Istituto di Materiali Speciali per Electtronica e Magnetismo del Consiglio Nazionale delle Ricerche, via Chiavari 18/A I-43100 Parma, Italy

Received 18 March 1993

Abstract. The magnetocrystalline anisotropy and the magnetic phase diagram of the pseudoternary $(Er_xHo_{1-x})_2Fe_{14}B$ were studied by using the singular point detection technique, thermomagnetic analysis, low-field AC and DC susceptibility and polar dependence of $M_\parallel$ and $M_\perp$ measurements. The competition among the different anisotropic contributions gives rise to a complex magnetic phase diagram in which a complete axis–cone–plane spin-reorientation transition is observed with decreasing temperature for $x > 0.6$. A linear composition dependence of the anisotropy was found in the temperature range 200–293 K, which constitutes an indication of the single-ion origin for the anisotropy in these compounds.

A microscopic single-ion crystal electric mean-field model has been used in order to explain the origin of the spontaneous spin-reorientation transitions as well as the thermal dependence of the measured anisotropy fields for all concentrations.

1. Introduction

The tetragonal $R_2Fe_{14}B$ intermetallic compounds constitute the basis of the new permanent magnets and also provide ideal systems in order to investigate the complex interplay of magnetic exchange and crystal electric field (CEF) interactions (Mitchell *et al* 1989, Herbst 1991). In these compounds the anisotropic behaviour at high temperatures is driven basically by the Fe sublattice which presents a uniaxial anisotropy, although its origin is not very well known due to the itinerant nature of the 3d electrons (Givord *et al* 1984, Bolzoni *et al* 1987). Nevertheless, a common feature of all the compounds in this series has been very well established: all of them present uniaxial anisotropy above room temperature. As a consequence, in this range of temperature all of the magnetic rare-earth and iron sublattices are aligned along the c axis. Usually the Fe sublattice anisotropy is taken as the anisotropy found for $Y_2Fe_{14}B$.

The spin reorientation transition at 60 K observed in $Ho_2Fe_{14}B$ is ascribed to the competition between the second- and higher-order CEF terms of the Ho^{3+} ions (Hirosawa *et al* 1986). In this transition the easy magnetization direction rotates from the c axis to an intermediate direction between the c axis and the basal plane within the $(1\bar{1}0)$ plane. This final magnetic structure will be named the easy cone structure in the following for

§ Present address: Dipartamento di Fisica, Universita di Parma, Vialle delle Science, 43 100 Parma, Italy.

0953-8984/93/315637+12$07.50

the sake of simplicity. On the other hand, the negative value of the second-order Stevens coefficient α_J favours the c axis as easy magnetization direction for temperatures above the spin reorientation transition, the Ho and Fe sublattice anisotropies being in accordance. On the contrary, the Er^{3+} ions have positive α_J Stevens coefficient and consequently a planar contribution to the anisotropy from the R sublattice should be expected in $Er_2Fe_{14}B$. This all gives rise to a competition between the planar and uniaxial anisotropies of the Er and Fe sublattices respectively, resulting in an easy-axis to plane spin-reorientation transition below 322 K, which takes place in the (010) plane (Hirosawa and Sagawa 1985, Hirosawa *et al* 1986).

As a consequence of the competition among the different contributions (Ho, Er, Fe) to the magnetic anisotropy, the occurrence of peculiar features is expected in the mixed system $(Er_xHo_{1-x})_2Fe_{14}B$. In similar compounds, such as $(Er_xNd_{1-x})_2Fe_{14}B$ (Ibarra *et al* 1988, Del Moral *et al* 1989), a new unexpected spin reorientation transition from an easy-cone magnetic structure 1 to another easy-cone structure 2 was found. It was also established the presence of different types of first-order magnetization process (Marusi *et al* 1990). A complex magnetic phase diagram was also found in $(Er_xDy_{1-x})_2Fe_{14}B$ (Ibarra *et al* 1989, Rechenberg *et al* 1987, Niarchos and Simopoulos 1986) and $(Er_xPr_{1-x})_2Fe_{14}B$ (Boltich *et al* 1987) and this was accounted for in the framework of a microscopic model by using second- and fourth-order CEF terms for Er–Dy compounds and only second-order terms for Er–Pr.

The characterization of the CEF and exchange interactions that the R ion experiences in the $R_2Fe_{14}B$ intermetallic compounds is not a trivial problem. A large effort of different researchers and groups has been undertaken in order to explain the magnetic behaviour observed, using either macroscopic or microscopic experimental techniques (Ibarra *et al* 1989, Rechenberg *et al* 1987, Niarchos and Simopoulos 1986, Boltich *et al* 1987, Boltich 1988, Givord *et al* 1988, Cadogan *et al* 1988, Yamada *et al* 1988, Radwanski and Franse 1989, Loewenhaupt *et al* 1990). The microscopic models used allow the intensity of the CEF interaction and the molecular field to be determined. The aim of the present investigation is to show that under the hypothesis of a single-ion origin for the anisotropy of the rare earth it is possible to give a reliable description of the magnetocrystalline anisotropy in these substituted $(Er_xHo_{1-x})_2Fe_{14}B$ rare-earth intermetallic compounds. This procedure represents a rather strict test for the proposed CEF and exchange parameters. A preliminary work (Marquina *et al* 1989), on the compound $(Er_{0.6}Ho_{0.4})_2Fe_{14}B$, revealed Er–Ho as a very interesting series to be studied.

2. Experimental details and results

Polycrystalline samples of composition $(Er_xHo_{1-x})_2Fe_{14}B$ ($x = 0$, 0.1, 0.2, 0.3, 0.4, 0.6, 0.65, 0.75, 0.8, 1) were prepared by melting high-purity elements in an arc furnace, and homogenized under vacuum for seven days at 870°C. The phase analysis was performed using both x-ray diffraction and the more sensitive thermomagnetic analysis (TMA). This latter technique was also used to measure the Curie temperature (T_C) which was found to increase linearly from $Er_2Fe_{14}B$ to $Ho_2Fe_{14}B$. X-ray measurements confirmed that the samples are single phase having the expected tetragonal crystal structure. However, the presence of some α-iron ($T_C = 770$°C) was detected by TMA in all samples. It is worth noticing that the presence of such a secondary phase is so small that it does not affect the magnetic and anisotropic properties of our samples.

2.1. Low-field magnetic susceptibility

High-sensitivity low-field AC susceptibility and magnetization measurements were performed in the range of temperature 3.5–300 K. This technique has been incorporated in our investigations because of the sensitivity of the dynamic susceptibility to the critical fluctuations which take place in the neighbourhood of the spin-reorientation transition temperature (Ibarra *et al* 1988, Del Moral *et al* 1989). The AC initial magnetic susceptibility was measured using a modified mutual inductance Hartshorn bridge operating at a frequency of 15 Hz. The current at the primary was such as to produce an AC magnetic field of 35 mOe peak value and the samples were free powders. The magnetization measurements were made on magnetically aligned samples using an extraction magnetometer (Del Moral *et al* 1988, Joven *et al* 1990) and a vibrating sample magnetometer. The temperature dependence of the low-field AC susceptibility for some of the measured compounds is displayed in figure 1. Large peak-like anomalies are observed at temperatures in which the spin-reorientation processes start to take place. This is a consequence of the weakening of the overall magnetic anisotropy because of the interplay of different competing magnetic anisotropies. The strong fluctuations associated with the critical character of this transition are the origin of such an anomalous behaviour (Del Moral *et al* 1989). As is quite clear, more than one anomaly is observed for intermediate concentrations; some of them are well defined peak-shaped anomalies while others appear as shoulder-like anomalies. The most important aspect of these measurements is the confirmation of the existence of a cone 1–cone 2 spin-reorientation transition, which was first observed in $(Er_xNd_{1-x})_2Fe_{14}B$ (Ibarra *et al* 1988). The peaks observed at higher temperatures (T_{SR1}) for the different concentrations, figure 1, correspond to the axis–cone 1 spin-reorientation transition. The temperature at which the cone 1–cone 2 transition takes place is represented as T_{SR2}.

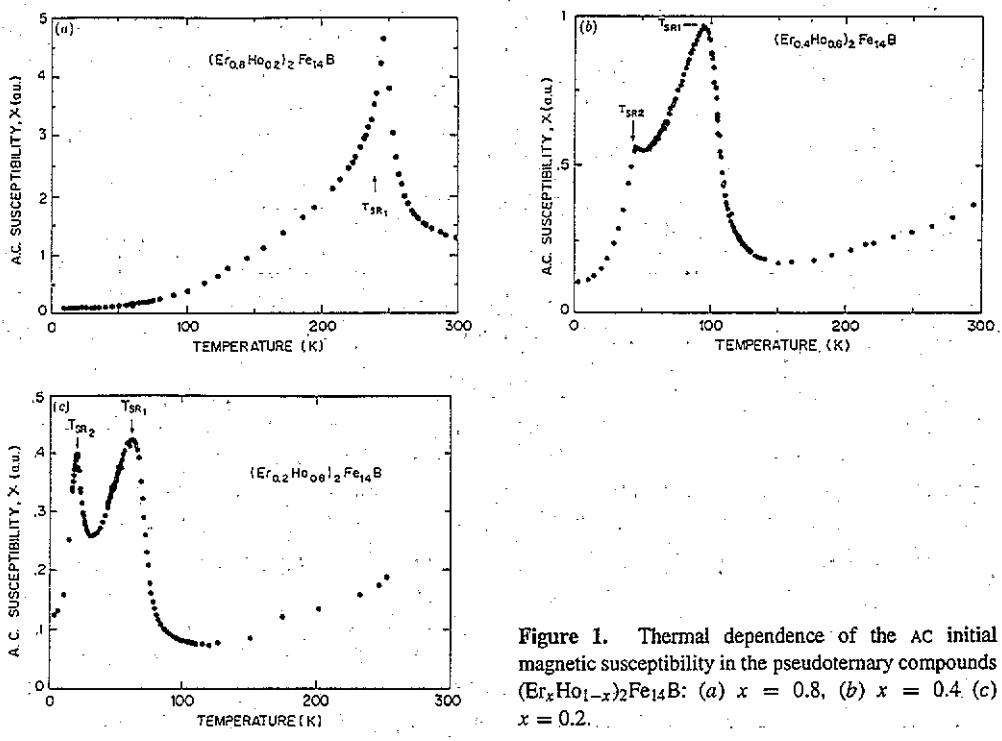

Figure 1. Thermal dependence of the AC initial magnetic susceptibility in the pseudoternary compounds $(Er_xHo_{1-x})_2Fe_{14}B$: (*a*) $x = 0.8$, (*b*) $x = 0.4$ (*c*) $x = 0.2$.

2.2. *Polar dependence of the parallel and perpendicular components of the magnetization to the applied magnetic field*

From the aforementioned AC initial magnetic susceptibility measurements we can delimit the different regions in the magnetic phase diagram. Nevertheless, additional experimental information is necessary to test the nature of this transition and confirm the observed complex magnetic behaviour. The polar dependence of the parallel $M_{\parallel}$ and perpendicular $M_{\perp}$ components of the magnetization allows determination of the orientation of the easy magnetization direction either in a single crystal or in a magnetically aligned sample. In our case, because of the difficulty of obtaining single-crystalline materials we have used magnetically aligned samples. These samples, due to the high uniaxial anisotropy near room temperature, can be magnetically oriented. For such a purpose we prepared a fine powder ($< 40\ \mu$m), which was aligned under a steady magnetic field of 6 kOe and compacted using epoxy resin. The orientations of the samples were carefully tested by measuring the magnetization parallel and perpendicular to the c axis at room temperature. The polar dependence of $M_{\parallel}$ and $M_{\perp}$ was measured using disc-shaped samples with the easy c axis and any direction of the basal plane in the plane of the disc surface. We have used a modified and completely automated extraction magnetometer, in which it is possible to measure simultaneously both magnetization components as function of the angle θ with respect to the applied magnetic field. Details of the instrument used have been reported elsewhere (Del Moral *et al* 1988, Joven *et al* 1990). In a typical curve we obtain a maximum for $M_{\parallel}$ when the magnetic field is applied along the easy direction and a minimum when it is applied along a hard direction. Moreover, $M_{\perp}$ is proportional to the torque that the sample experiences under an applied magnetic field. This torque is zero when the magnetic field is applied along either an easy magnetization direction or a major symmetry direction. As an example in figure 2 we display the results obtained for $x = 0.8$ at temperatures which correspond to the uniaxial (a), conical (b) and planar (c) regions of this sample. Using this technique in all compounds of this series we have been able to determine the thermal dependence of the spin-reorientation cone angle. The results obtained are represented in figure 3.

2.3. *Anisotropy field*

The well known singular point detection (SPD) technique (Asti and Rinaldi 1972, 1974) has been used in order to measure the anisotropy field H_A using high pulsed magnetic fields up to 300 kOe. This technique allows a fast and reliable determination of H_A to be made in both easy-axis and easy-plane polycrystalline materials (Pareti 1988). Magnetically aligned samples of compounds that present complex intermediate magnetic structures have also been successfully studied using this technique. The anisotropy field will be considered as the magnetic field which is required to saturate the sample along the hard direction in which the field is applied. We will indicate by H_A^P the anisotropy field when the magnetic field is applied along a direction on the basal plane and by H_A^C the anisotropy field measured when the field is applied along the c axis. In the region of temperature in which a sample has the easy-cone structure, both anisotropy fields can be measured. To give an expression for H_A^C and H_A^P the anisotropy and Zeeman energies for a uniaxial system can be considered.

$$E = K_1 \sin^2\theta + K_2 \sin^4\theta + \ldots - \boldsymbol{H} \cdot \boldsymbol{M}_s \tag{1}$$

where K_i are the phenomenological anisotropy energy constants, $\boldsymbol{H}$ is the applied magnetic field and M_s the saturation magnetization. Consequently the anisotropy fields H_A^P and H_A^C

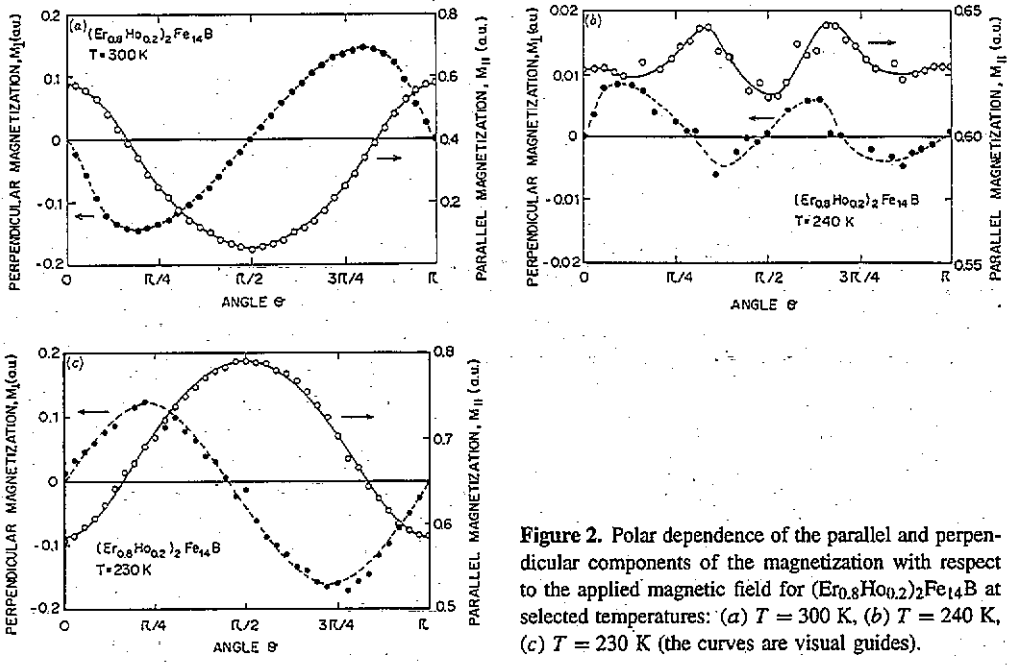

Figure 2. Polar dependence of the parallel and perpendicular components of the magnetization with respect to the applied magnetic field for $(Er_{0.8}Ho_{0.2})_2Fe_{14}B$ at selected temperatures: (*a*) $T = 300$ K, (*b*) $T = 240$ K, (*c*) $T = 230$ K (the curves are visual guides).

are given by

$$H_A^C = 2K_1/M_s \tag{2a}$$

$$H_A^P = 2(K_1 + 2K_2 + 3K_3)/M_s. \tag{2b}$$

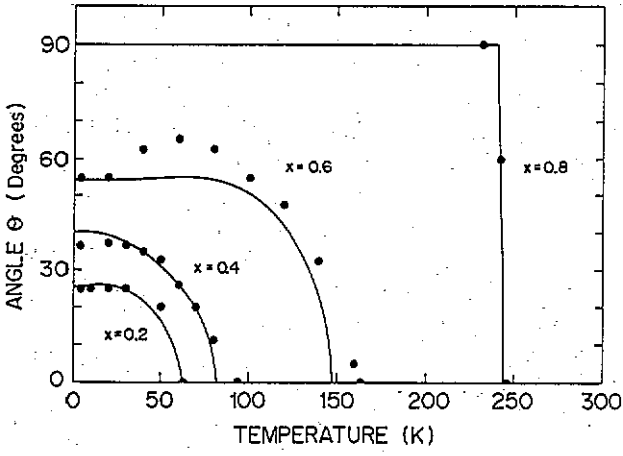

Figure 3. Thermal dependence of the spin-reorientation angle θ for the compounds $(Er_xHo_{1-x})_2Fe_{14}B$: ●, experimental results; ——, theoretical prediction.

Both anisotropy fields were accurately measured using the SPD technique in magnetically aligned samples and their temperature dependence is reported in figures 4 and 7.

The measured composition and temperature dependence of the anisotropy fields confirms that in the mixed systems, a compensation of the different competing magnetic anisotropies

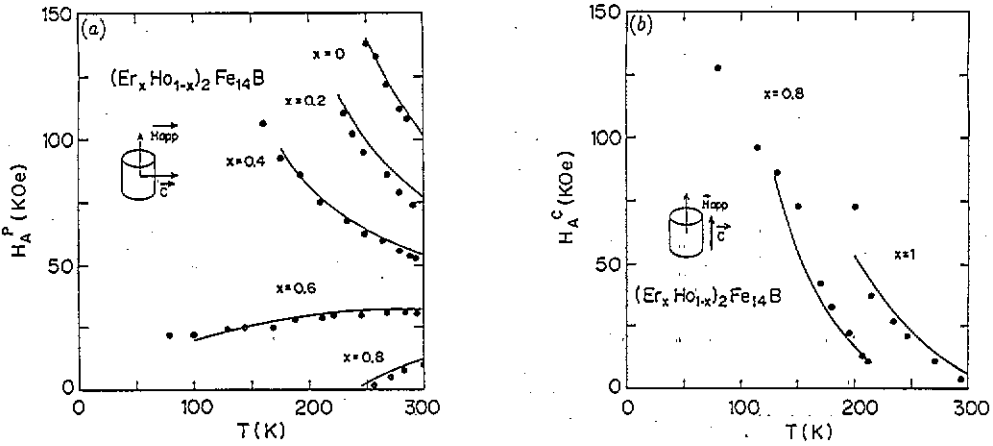

Figure 4. Temprature dependence of the anisotropy field for different compositions of $(Er_xHo_{1-x})_2Fe_{14}B$. The curves are theoretical predictions. (*a*) $H_A^P = (2K_1 + 4K_2 + \ldots)/M_s$; (*b*) $H_A^C = 2K_1/M_s$.

exists. This fact is clear from the results in figure 4(*a*) where the dramatic variation in magnitude and temperature dependence of H_A^P can be observed. When the easy magnetization direction is not along the *c* axis it is possible to obtain the values for H_A^C; thus the observed temperature behaviour allows the thermal variation of K_1 to be obtained. An almost linear composition dependence is observed for the room temperature value of the overall anisotropy constant $K = (K_1 + 2K_2 + 3K_3) = H_A^P M_s/2$ (figure 5). The values obtained at room temperature for H_A^P are given in table 1. Such a linearity is maintained down to 200 K (figure 5). At lower temperatures the comparison cannot be made because of the difficulty in measuring the anisotropy in a specimen with high Ho concentration. This difficulty is due to the large increase of H_A^P and to the smoother approach to saturation (demonstrated by the increasing large positive K_2) which implies a reduction of the SPD peak amplitude (Asti and Rinaldi 1974). It has to be noted that for easy-plane compounds the anisotropy constant K is K_1, whilst for easy-axis compounds $K = K_1 + 2K_2 + 3K_3 + \ldots$. The observed linear composition dependence of the magnetic anisotropy in the temperature interval 293–200 K, shown in figure 5, implies that there is no significant contribution to the magnetocrystalline anisotropy due to the term $2K_2 + 3K_3$ in this temperature region. The different anisotropic contributions from Er, Ho and Fe magnetic sublattices seem to add linearly to give the resultant macroscopic anisotropy. However non-linear effects could be expected at lower temperatures (Pareti 1988, Sarkis and Cullen 1982, Rinaldi and Pareti 1979, Asti *et al* 1987).

For the compositions $x = 0.8$ and 1, in the temperature range where they have the easy-plane structure, using the SPD technique, it is possible to measure the anisotropy field in the basal plane ($H_A^{P'}$). This is the field needed to rotate the magnetization vector within the basal plane from the easy (100) to the hard (110) in-plane direction. The observed temperature variation of $H_A^{P'}$ is reported in figure 6 for $x = 0.8$ and 1. A complete picture of the temperature variation of the various anisotropy fields is given for $x = 0.8$ in figure 7. From the analysis of the anisotropy energy of a tetragonal system

$$E = K_1 \sin^2\theta + (K_2 + K_2' \cos 4\phi) \sin^4\theta + (K_3 + K_3' \cos 4\phi) \sin^6\theta \qquad (3)$$

the expression $H_A^{P'} = 16(K_2' + K_3')/M_s$ is derived for the anisotropy field in the basal plane. From the measured values of the anisotropy fields, it can be deduced that these in-plane

Table 1. Anisotropy field in kOe and anisotropy constant in erg cm^{-3} at room temperature for different compositions of $(Er_xHo_{1-x})_2Fe_{14}B$. The spin-reorientation transition temperatures T_{SR} are given in Kelvin. C1, C2 and P respectively represent cone 1, cone 2 and planar magnetic phases.

	x									
	0	0.1	0.2	0.3	0.4	0.6	0.65	0.75	0.8	1
H_A^P	108.9	92.5	74.9	66.7	53.1	30.9	25.9	15.3	10.4	—
K (10^6)	34.7	29.7	24.7	22.3	18.1	10.9	9.2	5.5	3.8	1.48
T_{SR1} (K)	58		68	80	100	165	183	227	248	315
					110[a]	166[a]	187[a]	239[a]	247[a]	320[a]
T_{SR2} (K)			22	36	45	41	133[a]	207[a]	237[a]	(320)[a]
							140			
			C1–C2	C1–C2	C1–C2	C1–C2	C–P	C–P	C–P	C–P

[a] T_{SR} measured by DC susceptibility.

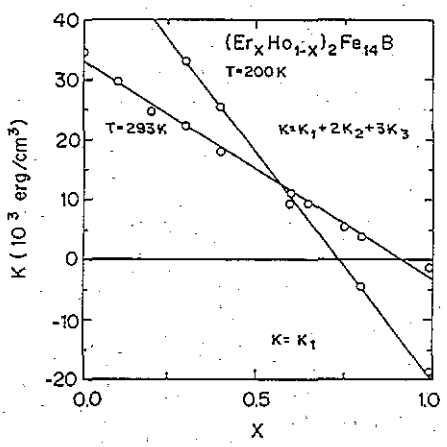

Figure 5. Composition dependence of the phenomenological anisotropy constant at 200 K and 293 K.

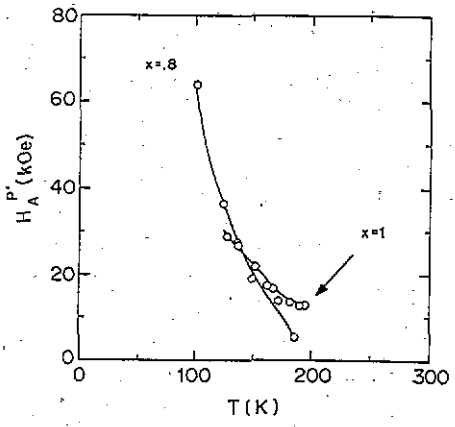

Figure 6. Temperature dependence of the anisotropy field $H_A^{P'}$ in the basal plane in $(Er_xHo_{1-x})_2Fe_{14}B$ for $x = 0.8$ and 1. The curves are visual guides.

high-order anisotropy constants are about one order of magnitude smaller than the uniaxial anisotropy constants.

3. Magnetic phase diagram

A small variation of 2.5% was observed in the T_C values between the extreme concentrations $Er_2Fe_{14}B$ (543 K) and $Ho_2Fe_{14}B$ (557 K) compounds. This variation was observed to be linear through the series. The magnetically ordered region for temperatures above room temperature is characterized by the dominance of the 3d band uniaxial anisotropy, but below this region of temperature, several zones in the magnetic phase diagram can be distinguished. The complex magnetic phase diagram of the Ho–Er system is shown in figure 8 (see also table 1). The composition range $x > 0.6$ is characterized by a complete spin-reorientation transition of the easy magnetization direction from the c axis to a cone and to the basal plane. The temperature value of the transition axis–cone 1 (T_{SR1}) decreases linearly with increasing Ho content. The value of the cone 1–plane transition temperature (T_{SR2} for

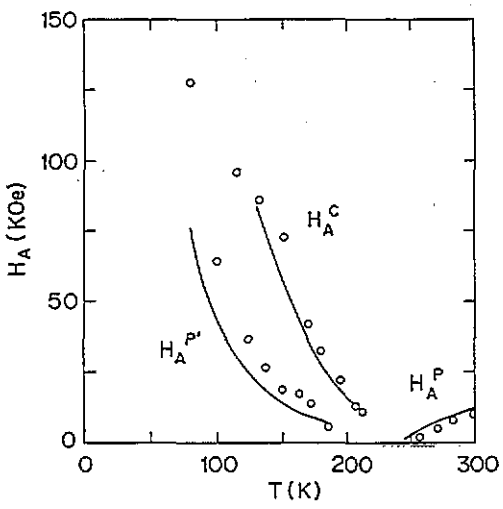

Figure 7. Temperature dependence of the different anisotropy fields H_A^C, H_A^P and $H_A^{P'}$ in $(Er_{0.8}Ho_{0.2})_2Fe_{14}B$. The curves are theoretical predictions.

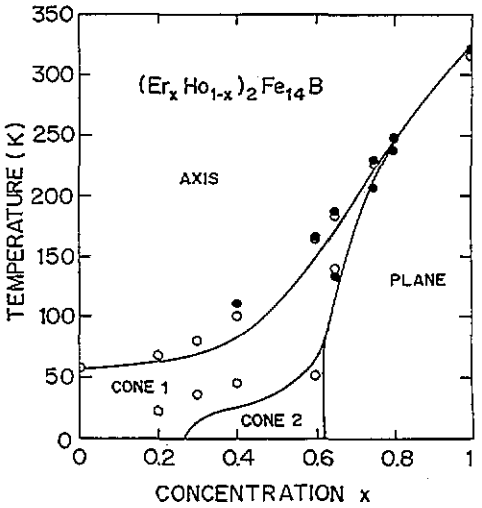

Figure 8. Magnetic phase diagram of the $(Er_xHo_{1-x})_2Fe_{14}B$ system obtained from AC (○) and DC (●) susceptibility measurements. ----, visual guides; ——, theoretical calculations.

$x > 0.6$) decreases as well, but more rapidly, in such a way that the temperature interval in which the samples have the easy cone structure increases with increasing Ho concentration. The character of the described spin-reorientation transition, in this composition range, can be well interpreted simply by considering the competition between the anisotropies of Fe (uniaxial) and Er (planar). The effect of Ho substitution consists of an enhancement of the overall uniaxial anisotropy and a reduction of the planar contribution (lower Er content).

The second spin-reorientation transition, which takes place at T_{SR2} for $0.1 < x \leqslant 0.6$, is not a cone–plane but a magnetic phase transition between two conical magnetic structures (cone 1 and cone 2) in which critical fluctuations between two different cone angle values occur. These phenomena have been also observed and extensively characterized in the isomorphous series $(Er_xNd_{1-x})_2Fe_{14}B$ (Ibarra *et al* 1988, Del Moral *et al* 1989). The value of T_{SR2} and the cone angle at 4 K decrease with increasing Ho content. No second spin-reorientation transition was observed for $x < 0.1$.

The axis–cone reorientation is still interpretable in terms of uniaxial versus planar competition. However, the cone 1–cone 2 transition, which takes place at $T < 60$ K for $0.1 < x \leqslant 0.6$, is the result of a rather more complex balance between the anisotropic contributions of Ho (which is conical in this temperature range) and Er (which is planar). In addition, the plane in which the easy magnetization rotates from the *c* axis toward the basal plane should change along the series as a consequence of the balance between the in-plane competing anisotropic contributions.

4. Microscopic model

The explanation of the anisotropic and magnetic behaviour of the series $(Er_xHo_{1-x})_2Fe_{14}B$ was undertaken on the basis of a single-ion origin for the anisotropy of the rare-earth magnetic sublattices. The Stevens operator formalism was used in order to account for the

electrostatic interaction of the rare-earth ions with the electrostatic surrounding. The matrix elements of these operators were obtained within the spin orbital $|L, S, J, M_J\rangle$ subspace. The polarization of the ground-state wave function by the first excited spin orbital level was neglected. This assumption is in accordance with the magnitude of the splitting of the ground-state degeneracy by the exchange and CEF interaction. For the point symmetry of the rare earth in this compound the CEF Hamiltonian can be written

$$H^{\mathrm{R}}_{\mathrm{CEF}}(i) = B^0_2(i)O^0_2 + B^{-2}_2(i)O^{-2}_2 + B^0_4(i)O^0_4 + B^{-2}_4(i)O^{-2}_4 + B^4_4(i)O^4_4 + B^0_6(i)O^0_6 + B^{-2}_6(i)O^{-2}_6 + B^4_6(i)O^4_6 + B^{-6}_6(i)O^{-6}_6 \tag{4}$$

where i denotes one of the four possible sites that the R^{3+} ion can occupy in this structure ($i = f_1, f_2, g_1$ and g_2). O^m_n are the Stevens operators and B^m_n the CEF parameters, which are given by

$$B^m_n(i) = \theta_n \langle r^n \rangle A^m_n(i) \tag{5}$$

where θ_n are the Stevens coefficients α, β, and γ for $n = 1$, 2 and 3 respectively. $\langle r^n \rangle$ is the average of r^n over the radial part of the wave function of the 4f electrons. $A^m_n(i)$ are the coefficients of the spherical harmonics which describe the crystal electric potential. We shall assume $A^m_n(\mathrm{f})$ and $A^m_n(\mathrm{g})$ to be different and also $A^{-2}_4(i) = A^{-2}_6(i) = A^{-6}_6(i) = 0$.

The exchange Hamiltonian which represents the magnetic bilinear exchange interaction between the rare-earth and iron magnetic sublattices will be considered within the molecular field approximation:

$$H^{\mathrm{R}}_{\mathrm{ex}}(i) = g_J \mu_{\mathrm{B}} \boldsymbol{J}^{\mathrm{R}} \cdot \boldsymbol{H}^{\mathrm{R}}_{\mathrm{mol}}(i) \tag{6}$$

where $g_J \mu_{\mathrm{B}} \boldsymbol{J}^{\mathrm{R}}$ is the rare-earth magnetic moment and $\boldsymbol{H}^{\mathrm{R}}_{\mathrm{mol}}$ is the effective molecular field. In the present model we only consider the molecular field originated by the ferromagnetic exchange coupling between the rare-earth and iron sublattices. We assume the R–R and the R–R′ indirect exchange interaction to be negligible and the Fe–Fe exchange interaction irrelevant in order to study the anisotropic behaviour, because such an interaction only introduces an angular-independent self-energy contribution to the free energy of the system. In expression (6) we have considered $H_{\mathrm{mol}} = [2(g_J - 1)/g_J]H_{\mathrm{ex}}$ where H_{ex} is the exchange field describing the spin angular momentum 4f–3d exchange. The thermal evolution was obtained by using $H_{\mathrm{mol}}(T) = H_{\mathrm{mol}}(0)(M_{\mathrm{Fe}}(T)/M_{\mathrm{Fe}}(0))$.

The free energy for each R magnetic sublattice is obtained from the partition function $Z(i) = \sum_n \exp(-E_n(i)/k_{\mathrm{B}}T)$ where E_n are eigenvalues of the Hamiltonian $H^{\mathrm{R}}_{\mathrm{CEF}}(i) + H^{\mathrm{R}}_{\mathrm{ex}}(i)$. The total free energy $F^{\mathrm{R}}(\theta, \phi, T)$ for the rare-earth sublattice when the molecular field makes an angle θ with the c axis [001] and an angle ϕ with the a axis [100] is given by

$$F^{\mathrm{R}} = -xk_{\mathrm{B}}T \sum_{i=1}^{4} \ln Z(i)^{\mathrm{Er}^{3+}} - (1-x)k_{\mathrm{B}}T \sum_{i=1}^{4} \ln Z(i)^{\mathrm{Ho}^{3+}}. \tag{7}$$

The total free energy for the system is calculated introducing the uniaxial iron sublattice anisotropy energy $E_{\mathrm{k}} = K_1(T)\sin^2\theta$:

$$F(\theta, \phi, T) = F^{\mathrm{R}}(\theta, \phi, T) + E_{\mathrm{k}}(\theta, T). \tag{8}$$

4.1. Spin reorientation

We have used the aforementioned model in order to account for the spin-reorientation transition phenomena which take place at T_{SR1} in this series of compounds. The spin-reorientation temperature T_{SR1} has been obtained from the numerical minimization of expression (8). This temperature has been identified as the temperature at which the effective easy-magnetization direction rotates away from the c axis. When the minimum for the free energy takes place for $\theta \neq 0$ a non-collinear orientation of the magnetization of the different magnetic sublattices occurs.

The orientation and amplitude of the effective magnetic moment for each magnetic sublattice were obtained by using the eigenvalues and eigenvectors of the Hamiltonian $(H^{R}_{CEF}(i) + H^{R}_{ex}(i))$. The resulting effective magnetic moment is calculated as $\mu = \sum_{i=1}^{4} \mu_{Er}(i) + \sum_{i=1}^{4} \mu_{Ho}(i) + \mu_{Fe}$. The rare-earth effective magnetic moment is calculated by using the expression

$$\mu_{R}(i) = -g_{J}\mu_{B}\langle J^{R}\rangle \tag{9}$$

where the thermal averages $\langle\rangle$ are calculated using the eigenvalues and eigenvectors $|n\rangle = \sum a_{nj}|J, M_J\rangle$ of the Hamiltonian $H^{R}(i)$, in the form

$$\langle J^{R}\rangle = \sum_{n}\langle n|J^{R}|n\rangle \exp\left(\frac{-E_n}{k_B T}\right) \Big/ \sum_{n} \exp\left(\frac{-E_n}{k_B T}\right). \tag{10}$$

A satisfactory explanation of our results for the spin-reorientation angle measured as described in this section is achieved. The results of our theoretical prediction are compared with the experimental results in figure 3. The CEF parameters and the molecular field values were taken from Givord *et al* (1988) and Cadogan *et al* (1988). From these calculations it has been possible to closely predict the T_{SR1} values of the spin-reorientation transitions which take place for high Er concentrations in the plane (010) ($\phi = 0$) and for low Er content in the plane ($1\bar{1}0$) ($\phi = \pi/2$). The model used also allowed the prediction of the cone 2 region in the phase diagram (see figure 8). The cone 1–cone 2 transitions correspond to a reorientation for a fix polar angle θ from $\phi = 0$ or $\phi = 45°$ to an intermediate value. As we already have mentioned, the cone 1–cone 2 spin-reorientation transition seems to be originated by the competition between the in-plane anisotropies of the Ho^{3+} and Er^{3+} ions. In fact for $Er_2Fe_{14}B$ the easy direction in the basal plane corresponds to the [100] direction and that for the $Ho_2Fe_{14}B$ corresponds to the [110] direction. These kinds of transition were first found in $(Er_xNd_{1-x})_2Fe_{14}B$ (Ibarra *et al* 1988, Del Moral *et al* 1989) and theoretically predicted by Cadogan and Li (1992). The calculated thermal dependence of the angle ϕ is represented in figure 9. From these calculations we predict that at the lowest temperatures the angle ϕ tends to a value of $25° < \phi < 30°$ for the intermediate concentrations ($0.2 \leqslant x \leqslant 0.7$).

4.2. Theoretical calculation of the anisotropy field

The exposed microscopic model has also been applied in order to explain the thermal dependence of the anisotropy field for the different compositions. The experimental results for H^{P}_{A} and H^{C}_{A} were obtained by using the SPD technique on magnetically aligned samples as described in section 2.3. In this new situation we need to determine the behaviour of the different magnetic sublattices under an applied magnetic field. For such a purpose we should consider the Zeeman contribution to the total Hamiltonian, which is given by

$$H^{R}_{Z}(i) = g\mu_{B}J^{R}(i)\cdot H. \tag{11}$$

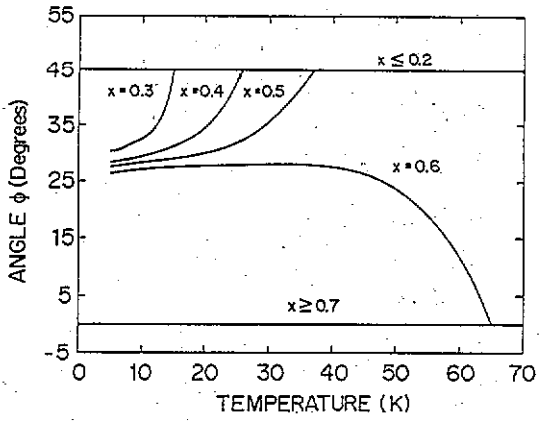

Figure 9. Calculated thermal dependence of the angle ϕ for the compounds $(Er_xHo_{1-x})_2Fe_{14}B$.

Using the total Hamiltonian $H(i) = H^R_{CEF}(i) + H^R_{ex}(i) + H_z(i)$ we have calculated the value of the angular dependence of the free energy using (8) for each concentration, temperature and value of the magnetic field. From these results we have calculated the amplitude and orientation of the effective total magnetic moment. The analysis of the calculated isotherms for a magnetic field applied along the c axis and along the a and b directions in the basal plane allowed us to obtain the H^C_A, H^P_A and $H^{P'}_A$ anisotropy fields respectively (Ibarra *et al* 1991). The results obtained are represented in figures 4 and 7.

5. Conclusion

Extensive experimental work has been carried out in order to obtain a deep insight into the anisotropic behaviour of the $(Er_xHo_{1-x})_2Fe_{14}B$ intermetallics. The magnetic behaviour below room temperature is a very useful guide for understanding the complex interplay between different basic interactions, i.e. CEF and exchange. The favourable situation in the case of these iron-rich intermetallics is the high Curie point and the high uniaxial anisotropy at room temperature. This feature allows the possibility for the small particles to be magnetically aligned. The substitution of Er by Ho in this series has the effect of modifying the balance between the different anisotropic interactions. This variation is controlled on the basis of the strong spatial localization of the magnetic 4f band, which makes the single-ion approximation quite suitable for this series of compounds. The complex magnetic phase diagram is composed of four different regions in the ordered regime (axis, cone 1, cone 2 and plane).

Despite the complex interplay of different interactions, a microscopic model can account for the thermal evolution of the effective spin-reorientation angle. A comparison with our macroscopic measurements for the whole series of compounds has allowed us to test the reliability of the CEF and exchange parameters. We have predicted the thermal dependence of the angle for the different magnetic sublattices during the spin-reorientation process. We have been able also to explain the thermal dependence of the different anisotropy fields for all the compounds in the series.

Acknowledgments

We are grateful to Professor A del Moral for many useful discussions. We also acknowledge the financial support of the Spanish CICYT through the grants PB92-0095 and MAT90-1103. This work is part of the Project BREU-68-C supported by the European Community.

References

Asti G, Bolzoni F and Pareti L 1987 *IEEE Trans. Magn.* **MAG-23** 2521
Asti G and Rinaldi S 1972 *Phys. Rev. Lett.* **28** 1584
—— 1974 *J. Appl. Phys.* **45** 3600
Boltich E B 1988 *J. Appl. Phys.* **63** 3124
Boltich E B, Pedziwiatr A T and Wallace W E 1987 *Mater. Res. Soc. Symp. Proc.* vol 96 (Pittsburgh, PA: Materials Research Society) p 119
Bolzoni F, Gavigan J P, Givord D, Li H S, Moze O and Pareti L 1987 *J. Magn. Magn. Mater.* **66** 158
Cadogan J M, Gavigan J P, Givord D and Li H S 1988 *J. Phys. F: Met. Phys.* **18** 779
Cadogan J M and Li H S 1992 *J. Magn. Magn. Mater.* **140** L20
Del Moral A, Ibarra M R, Marquina C, Arnaudas J I and Algarabel P A 1989 *Phys. Rev.* B **40** 7192
Del Moral A, Joven E, Ibarra M R, Arnaudas J I, Abell J S and Algarabel P A 1988 *J. Physique* **49** C8-449
Givord D, Li H S, Coey J M D, Gavigan J P, Yamada O, Maruyama H, Sagawa M and Hirosawa S 1988 *J. Appl. Phys.* **63** 3713
Givord D, Li H S and Perrier de la Bathie R 1984 *Solid State Commun.* **51** 857
Herbst J F 1991 *Rev. Mod. Phys.* **63** 819
Hirosawa S, Matsuura Y, Yamamoto H, Fijimura S and Sagawa M 1986 *J. Appl. Phys.* **59** 873
Hirosawa S and Sagawa M 1985 *Solid State Commun.* **54** 335
Ibarra M R, Algarabel P A, Marquina C, Arnaudas J I, Del Moral A, Pareti A, Moze O, Marusi G and Solzi M 1989 *Phys. Rev.* B **39** 7081
Ibarra M R, Marquina C, Algarabel P A, Arnaudas J I and Del Moral A 1988 *J. Appl. Phys.* **64** 5537
Ibarra M R, Morellon L, Algarabel P A and Moze O 1991 *Phys. Rev.* B **44** 9368
Joven E, Del Moral A and Arnaudas J I 1990 *J. Magn. Magn. Mater.* **83** 548
Loewenhaupt M, Sesnowsha I and Frick B 1990 *Phys. Rev.* B **42** 3866
Marquina C, Solzi M, Algarabel P A, Ibarra M R and Pareti L 1989 *Solid State Commun.* **72** 1167
Marusi G, Pareti L, Solzi M, Moze O, Paoluzi A, Ibarra M R, Arnaudas J I, Marquina C, Algarabel P A and Del Moral A 1990 *J. Magn. Magn. Mater.* **83** 133
Mitchell I V, Coey J M D, Givord D, Harris I R and Hanitsch R 1989 *Concerted European Action on Magnets* (London: Elsevier)
Niarchos D and Simopoulos A 1986 *Solid State Commun.* **59** 669
Pareti L 1988 *J. Physique* **49** C8-551
Radwanski R J and Franse J M M 1989 *J. Magn. Magn. Mater.* **80** 14
Rechenberg H R, Sanchez J P, Heritier P L and Fruchart R 1987 *Phys. Rev.* B **36** 1865
Rinaldi S and Pareti L 1979 *J. Appl. Phys.* **50** 7719
Sarkis A and Cullen E 1982 *Phys. Rev.* B **26** 3870
Yamada M, Kato H, Yamamoto H and Nakagawa Y 1988 *Phys. Rev.* B **38** 620